Development of New Catalytic Asymmetric Routes towards a Cost-Driving Building Block of Nirmatrelvir

Robert Szpera,[§*] Shanjun Huang,[§] Harriet A. M. Fenton,[§] William Waddington,[§] Adam E. S. Gymer,[§] Ian Moses,[§] Julia Buck,[§] Heather Ingram,[§] Steven J. Fussell,[§] Robert Walton,[§*] Charles S. Shanahan,[†*] Sarah L. Aleshire,[†] Juliana M. S. Robey,[†] Hanuman P. Kalmode,[†] Michel C. Nuckols,[†] Nageswara R. Kalikinidi,[‡] Venumadhav Janganati,[‡] Sipak Joyasawal,[‡] Chanaka M. Amarasekarage,[‡] Chris Senanayake,[‡] B. Frank Gupton[†]

§ Pfizer Worldwide Research and Development Discovery Park, Sandwich, Kent CT13 9NJ, U.K.
† Medicines for All Institute, Virginia Commonwealth University, Richmond, Virginia 23298, United States
‡ TCG GreenChem, Inc., Ewing, New Jersey, 08628, United States

KEYWORDS: nirmatrelvir, Paxlovid, asymmetric Michael addition, asymmetric conjugate addition, asymmetric 1,4-addition, API starting material, nitroacetate, benzophenone imine, chiral Lewis acid catalysis, copper, organocatalysis, bifunctional hydrogen-bond-donor catalysis

ABSTRACT: Nirmatrelvir is an inhibitor of SARS-CoV-2 main protease and is the active ingredient in Paxlovid™. Nirmatrelvir presents a significant synthetic challenge, in no small part due to a cost-driving lactam containing fragment with two stereogenic centers. Our goal was to help decrease the cost of nirmatrelvir, by developing a scalable low-cost synthesis of this fragment, avoiding use of cryogenic conditions reported in the initial route. Herein we disclose three catalytic asymmetric routes towards this fragment, via i) chiral Lewis acid (copper) catalysis, ii) chiral Brønsted base organocatalysis and iii) chiral bifunctional hydrogen-bond-donor organocatalysis.

INTRODUCTION

The COVID-19 pandemic created unprecedented levels of mobilization within the scientific community, aimed at developing therapies necessary to address the global emergency. To this end Pfizer developed Paxlovid™, which combines ritonavir, a strong CYP3A inhibitor, and nirmatrelvir, an inhibitor of SARS-CoV-2 main protease.[1] Paxlovid™ was given emergency use authorization for eligible patients by US FDA in November 2021,[2, 3] spurring significant development efforts to make the medication widely available globally. Within this context, Medicines for All Institute at Virginia Commonwealth University (VCU), working with TCG GreenChem Inc. and the Bill & Melinda Gates Foundation entered into a collaboration with Pfizer to attempt to develop lower-cost processes to produce nirmatrelvir.

The routes reported by Pfizer for preparing nirmatrelvir use fragments **1**, **2**, and **3** (Scheme 1A).[4-9] At the time this research was conducted, the high costs of these starting materials were a contributing factor to the limited global availability of nirmatrelvir and hence also Paxlovid™. One particular cost-driver of nirmatrelvir is lactam containing fragment **3**, the synthesis of which is challenging due to the presence of two nonadjacent stereocenters. The established strategy for preparing **3** utilizes a chiral pool approach; *N*-Boc-L-glutamic acid dimethyl ester is doubly deprotonated at -78 °C with excess LiHMDS, then treated with bromoacetonitrile resulting in diastereoselective alkylation (Scheme 1B).[10-12] While this method is elegant, it incurs cost in several ways, including the requirement for cryogenics conditions and excess LiHMDS, both of which are expensive on such large scales. Subsequent reports have studied modifications of this alkylation, however, none have addressed the limitations described above.[13, 14] Considering this, development of a non-cryogenic and scalable route for the synthesis of **3** is desirable.

An alternate option to the established chiral pool approach described above, would be to develop a catalytic asymmetric reaction to prepare fragment **3**, or precursors thereof (Scheme 1C). Such approaches may allow one to avoid use of cryogenic conditions and LiHMDS. In this paper, we describe our work to this end. We envisioned setting both α- and γ- stereocenters in a single step via an asymmetric (formal) Michael addition reaction between a lactam containing Michael acceptor **A** and an appropriate pronucleophile **B** (Scheme 1C). The Michael adduct **C** could then be converted into fragment **3** for the synthesis of nirmatrelvir.

*Scheme 1. A: Fragments in nirmatrelvir synthesis, B: previous approach to fragment **3**, C: asymmetric catalytic approach detailed in this report*

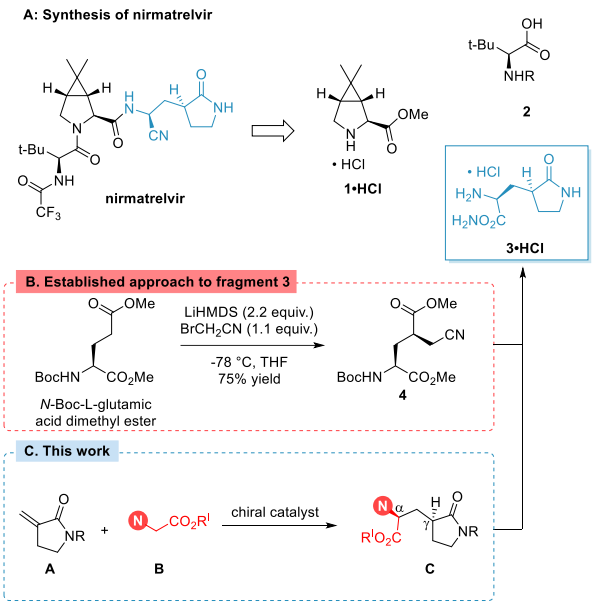

Scheme 2: Copper-catalysed asymmetric Michael Addition

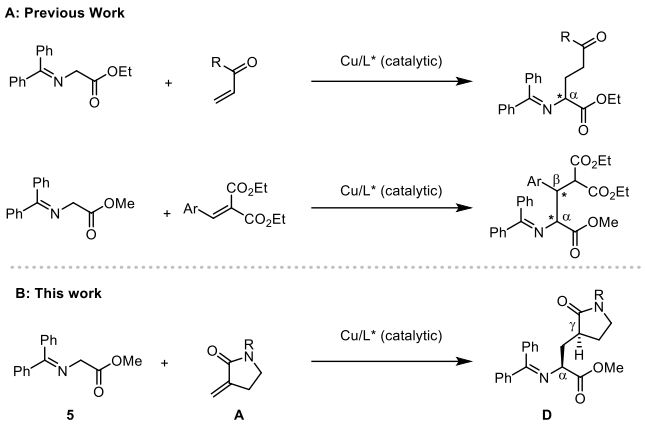

RESULTS & DISCUSSION

Copper Lewis Acid Catalysis

In the Pfizer Sandwich process chemistry labs, enantioselective Lewis acid catalysis was considered for setting the α- and γ-stereocentres of the target molecule **3**. There are various reports in the literature of enantioselective Michael additions of glycine imine esters to α,β-unsaturated electrophiles, catalysed by chiral copper complexes (Scheme 2A). Zajac and co-workers have reported Michael addition to enones,[15] Liu, Zhang and co-workers have reported addition to beta-trifluoromethyl enones,[16] and Arrayás, Carretero and co-workers have reported addition to gem-diactivated olefins.[17] Ferrocene based chiral phosphine ligands were used in each case. In addition to these studies, asymmetric Michael addition of glycine imines has also been reported under Ag(I) and Ca(II) catalysis.[18-21] We anticipated a similar strategy could be exploited for the enantioselective synthesis of **D** (Scheme 2B). While copper-catalysed asymmetric Michael addition has been exploited for setting both α- and β-stereocenters, we expected that achieving control of the more remote γ- stereocenter in **D** would be challenging.

Previous reports of copper mediated Michael-additions of glycine imine esters have used relatively activated enones and gem-diactivated alkenes as Michael acceptors.[15-17] We anticipated that the nature of the *N*-substituent of our Michael acceptor would be crucial in rendering it reactive towards **5**. We therefor assessed the reactivity of both NH and *N*-Boc activated Michael acceptors **6** and **7**. We also assessed reactivity both in the presence and absence of copper, to test for undesired background reactivity (Table 1). Reaction mixtures were analysed by SFC-MS, as hydrolysis of the benzophenone imine in both the pro-nucleophile **5** and product **9** was observed under our standard LC-MS methods. In addition, chiral SFC enabled separation of each of the four product stereoisomers for quantification of reaction stereoselectivity. Our initial experiments were conducted with the achiral ligand DPPF, and DBU as base. No product formation or starting material consumption was observed when NH Michael acceptor **6** was used, both in the presence and absence of the copper catalyst. In contrast, the more electrophilic *N*-Boc lactam **7** did undergo the desired reaction; 10% SFC area percent (SFC-AP) of a 1:1 mixture of product diastereomers was observed with DBU alone, while in the presence 1,1'-bis(diphenylphosphino)ferrocene (DPPF) and Cu(I), 97% SFC-AP of a 1.26 : 1 diastereomeric mixture was obtained, in favour of the desired diastereomer. These results suggested that copper could catalyse the reaction and had potential to control the diastereoselectivity. The observed reaction of **7** with DBU in the absence of copper suggested that screening of different bases would be necessary to avoid background reactivity which would result in reduced ee and DR. Glycine imine esters like **5** have also been reported to react in [2+3] cycloadditions under copper-catalysis to afford pyrrolidines,[22-24] however under the conditions tested we did not detect any formation of such species.

Table 1: Reactivity of NH and NBoc Michael acceptors under Cu-catalysis

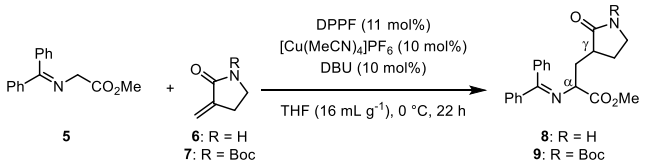

Entry	Cu/DPPF	R	Base	SFC-AP	DR
1	No	H	DBU	0	NA
2	Yes	H	DBU	0	NA
3	No	Boc	DBU	10	1 : 1
4	Yes	Boc	DBU	97	1.26 : 1

With proof of concept established using *N*-Boc Michael acceptor **7**, a high-throughput chiral ligand screen was executed to determine whether the reaction could be performed with the desired enantio- and diastereo-selectivity to afford (*S,S*)-**9** (Figure 1).

Literature precedence shows that ferrocene-based phosphine ligands have performed well in copper-catalysed Michael addition reactions of glycine imine esters,[15-17] and so the ligand screen was biased towards ligands of this class; JosiPhos, TaniaPhos, FOXAP, and FesulPhos ligands were all screened. Various bis-phosphines ligands were screened, including both those with chiral scaffolds, and those chiral at phosphorus. In addition, phorphoramidite, BOX and PyBox ligands were all screened.

Figure 1: Chiral ligand screen

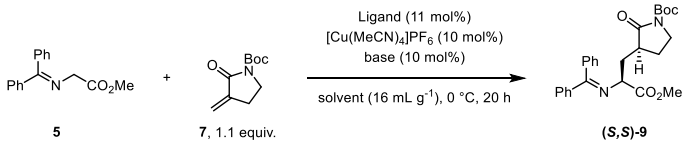

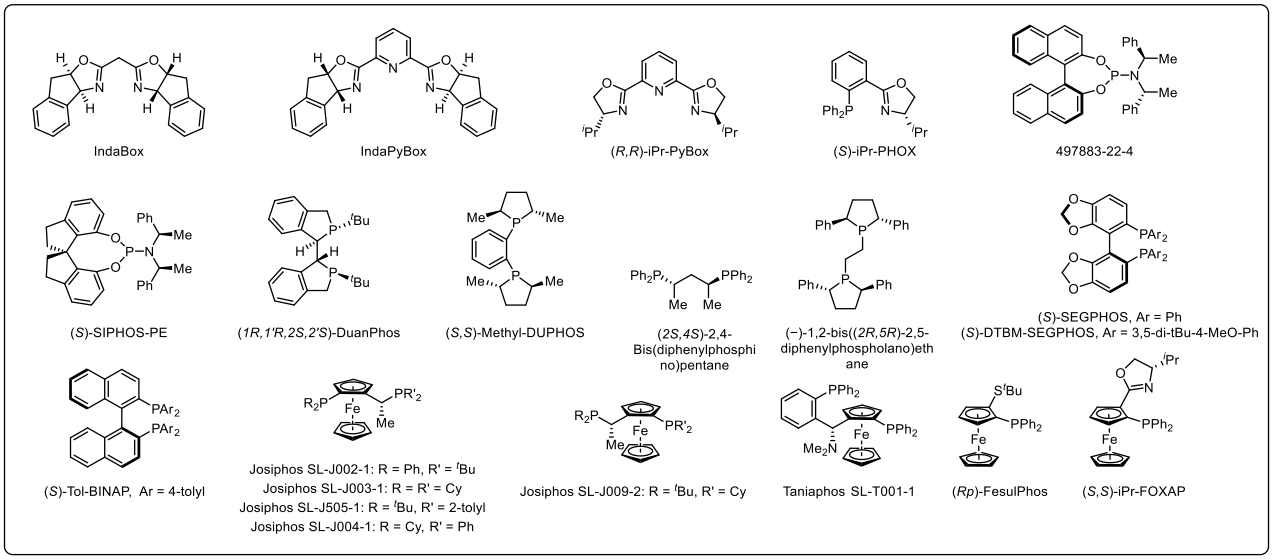

*The SFC-AP of all four product stereoisomers of **9** is plotted on the x-axis, and the stereoselectivity is plotted on the y-axis, as a fraction of **(S,S)-9** over all four possible stereoisomers of **9**. The datapoints are labeled with the ligand used. The shape of the spots corresponds to the solvent used, and the color corresponds to the base. See the legend in the top right of the figure for details.*

The ligands (*Rp*)-FesulPhos and (*S,S*)-iPr-FOXAP afforded the highest stereoselectivity for (*S,S*)-**9**, however the conversion with (*S,S*)-iPr-FOXAP was low. In contrast, the conversion with using (*Rp*)-FesulPhos with DBU was high. Similar analysis was performed for (*R,R*)-**9** – if this product stereoisomer was observed with good selectivity, the catalyst enantiomer could be switched to afford the desired product stereoisomer (*S,S*)-**9**. Excellent selectivity for the (*R,R*)-**9** was achieved using (−)-1,2-bis((*2R,5R*)-2,5-diphenylphospholano)ethane, however the conversion was low. Tol-BINAP was slightly less selective, but afforded much higher conversion. Nonetheless, (*Rp*)-FesulPhos performed best overall. Examining the effect of base, neither DBU nor DIPEA was preferred outright, with best base being dependent on the ligand used.

In preparation for reaction scale-up, we aimed to develop conditions with a lower catalyst loading. Using (*Rp*)-FesulPhos as ligand with 1 mol% copper loading, a range of bases were tested at both 0.5 and 0.1 equivalents, in addition to a small selection of solvents (Figure 2). Multiple of the conditions tested resulted in formation of the product with conversions and stereoselectivity similar to that observed employing 10 mol% of catalyst. Organic bases of various strengths were competent in the reaction, including DBU, MTDB, BTMG and tertiary amines DIPEA, pentamethylpiperidine (PMP), and DABCO. In contrast, weaker organic bases N-methyl-morpholine (NMM) and pyridine resulted in no conversion. Inorganic base K_3PO_4 was also competent, and to a lesser extent K_2CO_3. Weaker bases $NaHCO_3$, Na_2HPO_4, and KOAc were ineffective, resulting in very low or zero conversion. Use of NaOtBu resulted in significant formation of by-products. The reaction did not proceed in the absence of base.

In general, IPA resulted in significantly higher selectivity for the desired (*S,S*)-**9** than either toluene or THF. This was primarily due to the higher diastereomeric ratios (DRs) with IPA, but enantiomeric excesses (ees) were also higher. Whether 0.1 or 0.5 base equivalents performed better was dependent on the base strength; for DIPEA, DABCO and PMP, 0.5 equivalents performed better due to increased conversion, and higher DR. For stronger bases MTDB, DBU, BTMG and K_3PO_4, 0.1 equivalent was favoured, due to higher ee and DR, and reduced impurity formation. Overall, reactions with DIPEA (0.5 equivalents), MTDB (0.1 equivalent), and BTMG (0.1 equivalents) in IPA, and DABCO (0.5 equivalents in toluene) afforded the greatest stereoselectivity for desired product. While MTDB and BTMG afforded higher conversions, DIPEA was selected for continued optimisation due to its lower cost.

Figure 2: Base and solvent screening at 1 mol% copper loading

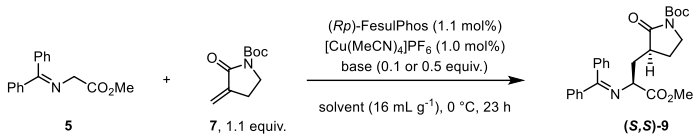

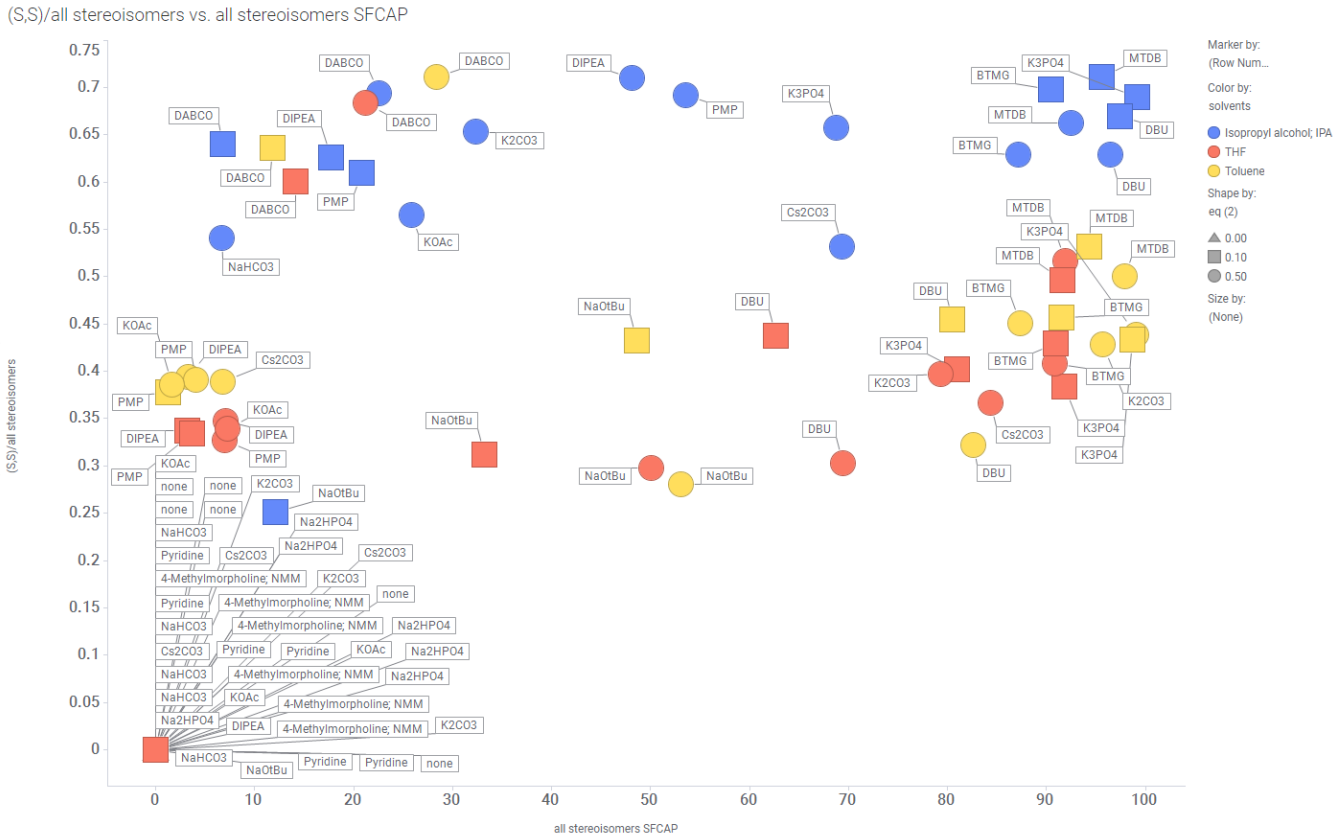

*The SFC-AP of all four product stereoisomers of **9** is plotted on the x-axis, and the stereoselectivity is plotted on the y-axis, as a fraction of **9** over all four possible stereoisomers of **9**. The datapoints are labeled with the base used. The shape of the spots corresponds to the equivalents of base used, and the color corresponds to the reaction solvent. See the legend in the top right of the figure for details.*

It was suspected that increasing the DIPEA equivalents beyond 0.5 would increase the conversion, based on results with 0.1 and 0.5 equivalents shown in Figure 2. A screen of various DIPEA equivalents was therefore carried out (Table 2). Increasing above 0.5 equivalents further increased the conversion and DR of the reaction, while maintaining a high ee of over 97%. The beneficial effect of increased DIPEA plateaued at around 2.5 equivalents.

Table 2: Optimization of DIPEA equivalents

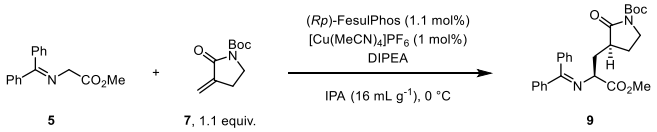

Entry	DIPEA Equiv.	SFC-AP	%ee (*S*,*S*)	DR	(*S*,*S*)/(all stereoisomer)
1	0.25	36	97.3	2.12 : 1	0.670
2	0.50	54	97.2	2.40 : 1	0.696
3	1.0	72	97.6	2.71 : 1	0.722
4	2.0	79	97.8	2.91 : 1	0.736
5	2.5	86	97.8	2.94 : 1	0.738
6	3.0	88	97.9	3.00 : 1	0.742
7	3.5	84	97.8	3.05 : 1	0.745

Due to the pronounced effect of solvent observed in the base/solvent screen in Figure 2, a further selection of solvents were tested (Table 3). Protic solvents (entries 1 to 4) afforded significantly higher conversions than all other solvents tested, which resulted in only very poor conversions. The nature of the alcohol had a large effect on the diastereoselectivity; both IPA and tAmOH favoured formation of the desired diastereomer, while MeOH and EtOH resulted in near equal quantities of both diastereomers. Nonetheless with all protic solvents, ee values remained above 90%. Similar optimisation of the base equivalents and solvent was also carried out using DBU as base, however the results were inferior to those obtained using DIPEA.

Which of the two stereocenters of **9** is set with a high level of control (>97% ee) and which was is with less control (~3 : 1 DR) was not determined, however based on prior literature, we believe that it is likely that it is the centre α to the ester that is set with high control.[15]

Table 3: Further solvent screening

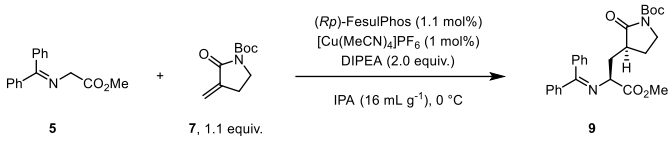

Entry	Solvent	SFC-AP	%ee (*S,S*)	DR	SS/(all stereoisomer)
1	IPA	79	97.8	2.91 : 1	0.736
2	MeOH	82	92.7	0.93 : 1	0.465
3	EtOH	91	95.7	0.85 : 1	0.449
4	tAmOH	51	97.9	2.56 : 1	0.712
5	THF	13	79.4	0.71 : 1	0.372
6	Toluene	8	85.3	0.82 : 1	0.418
7	Heptane	9	80.8	0.62 : 1	0.347
8	EtOAc	9	82.1	0.67 : 1	0.365

Next the kinetics of the reaction were investigated under different copper catalyst loadings (Figure 3). Automated reaction mixture sampling was performed using an Unchained Labs CM3. In this manner, concentration vs time profiles for four separate reactions could be acquired simultaneously and autonomously. Excellent reproducibility in kinetic data was seen between repeats of the same reaction conditions, as shown in Figure 3. These time-course experiments were conducted at 10 mL g^{-1} rather than 16 ml g^{-1}, which resulted in a faster reaction. Reducing the catalyst loading to 0.5 mol% resulted in a slower reaction, with significant starting material remaining after 24 hours. Contrarily, increasing the loading to 1.5 mol% resulted in the reaction reaching completion in roughly 10 hours instead of 20. An increase in DR was also observed as catalyst loading was increased, with 1.5 mol% copper giving ~3.35:1 selectivity for the desired diastereomer. The ee remained approximately unchanged with different catalyst loadings. Throughout the reactions, both the ee and DR of the product remain approximately constant. It is likely that increasing the concentration further would result in shorter still reaction durations. The purity of the Michael acceptor **7** was also found to impact the reaction rate, with less pure batches reacting more slowly and resulting in lower product DR. We speculated that the lower rate may be due to impurities binding to copper thus inhibiting catalysis.

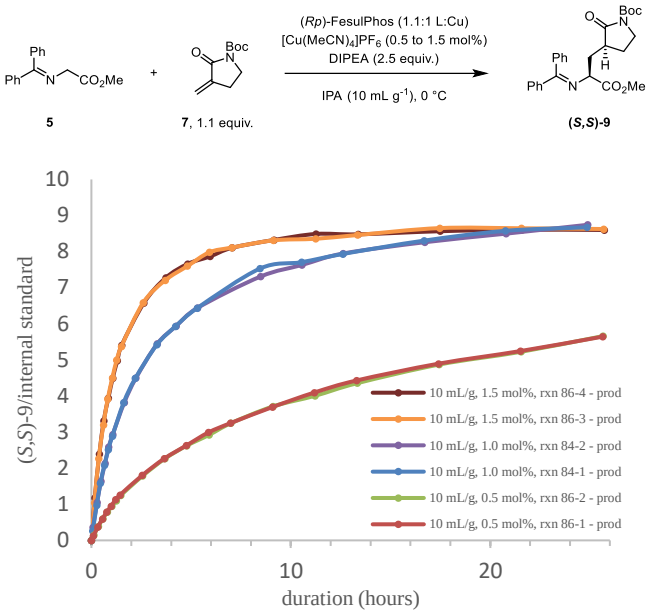

Figure 3: Time course data for with varying catalyst loadings

The optimisation experiments discussed hereto were conducted in a nitrogen filled glovebox with ~12 mg of **5** in 1 mL vials with magnetic stirring (time course experiments in 4 mL vials with ~126 mg of **5)**. To demonstrate the practicality and scalability of the chemistry, we sought to demonstrate the reaction in a manner relevant to process chemistry – outside of the glovebox with overhead stirring on multigram scale. Prior to scaling the reaction, process safety testing was carried out (see supporting information for further information). Differential scanning calorimetry (DSC) analysis of **7** showed an early endotherm from 59 °C, attributed to the compound melting, immediately followed by an exotherm at -280 J g^{-1} indicating a medium severity event.[25] This prompted further work to understand the reaction safety limits in more detail. DSC experiments performed on **5** and **9** showed some low thermal onsets, between -50 J g^{-1} to -100 J g^{-1} indicating low severity thermal events.[25] Further thermal stability assessment of the reaction mixture was conducted via a thermal screening unit (TSU), with no significant thermal onsets observed up to 248 °C, with gas observed from 150 °C attributed to thermal loss of the Boc protecting group. This analysis demonstrated that the intended conditions were safe for further scale-up.

Scale-up reactions were performed outside the glovebox on a bench, in an EasyMax reactor equipped with overhead stirring. Initial 1g reactions resulted in SFC profiles very similar to those observed in small scale optimisation studies. The ease of scale-up is likely in part due to the homogeneity of the reaction mixture. From a 1g experiment, product **9** was isolated *via* flash chromatography, in an isolated yield of 77% as a mixture of stereoisomers (3.73:1 DR by ^{1}H NMR, 99.0% ee). Due to the propensity of **9** to undergo hydrolysis, we sought to develop a telescoped procedure to isolate the deprotected product as the (-)-camphorsulphonic acid ((-)-CSA) salt **10·(-)-CSA**. However, DIPEA carried through from the copper-catalysed reaction resulted in difficulties isolating pure **10·(-)-CSA**, as the product was contaminated with DIPEA salts. We therefore investigated methods to remove DIPEA prior to deprotection / salt formation. Attempted precipitation of DIPEA from the reaction mixture as a salt using anhydrous HCl, $NaHSO_4.H_2O$ and TFA

all led to the undesired cleavage of the benzophenone imine. Instead, removal of DIPEA was achieved by passing the reaction mixture through a silica plug. Subsequent solvent swap into TBME and heating with (-)-CSA, followed by addition of acetone, afforded the product as a free flowing solid. Using this process, a 5 g scale reaction-deprotection-resolution was conducted, resulting in 67% isolated yield of **(*S,S*)-10·(-)-CSA** (Scheme 3). The use of (-)-CSA for the deprotection and salt formation enabled isolation of the product as a single diastereomer. Salts of **10** can be easily converted into nirmatrelvir fragment **3** via $MgSO_4$ mediated aminolysis.[8]

*Scheme 3: Scale-up of synthesis of **(S,S)-10·(-)-CSA** using asymmetric copper catalysis*

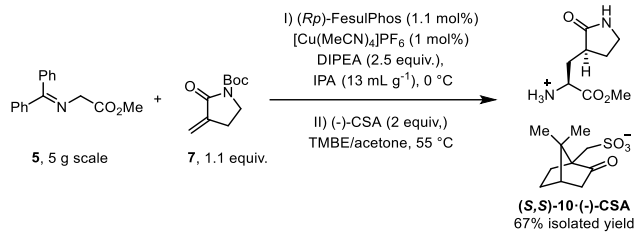

Chiral Brønsted Base Catalysis

While Pfizer Sandwich focused efforts on copper catalysis, Medicines for All Institute investigated leveraging chiral Brønsted base catalysis to control asymmetric Michael addition. The Lambert group have previously reported that chiral cyclopropeninime Brønsted bases such as **11** can catalyze the asymmetric Michael addition of glycine imines with various Michael acceptors (Scheme 4).[26, 27] No examples of α,β-unsaturated amides/imides as Michael acceptors were reported.

Scheme 4: Chiral Brønsted base catalysed Michael addition

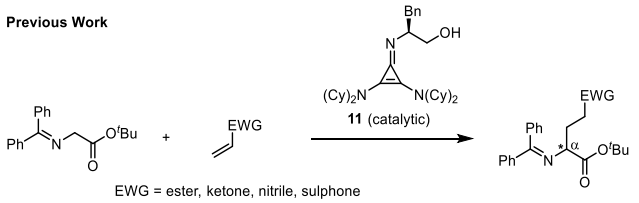

Investigation by the Medicines for All Institute began by exploring use of the chiral catalyst **11** for controlling asymmetric Michael addition between **5** and **7** (Table 4).[26, 27] These experiments were immediately fruitful and provided the desired product in good conversion and enantioselectivity, with selectivity for the desired diastereoisomer. Consistent with the observations of the Pfizer Sandwich team, reverse-phase HPLC methods rapidly hydrolyzed the benzophenone imine in **5** and the product **9**. The primary amine hydrolyzed product (**19,** Scheme 8) was therefor used to quantify reaction diastereoselectivity via LC-MS. Additional minor peaks were also observed by LC-MS, which were speculated to arise through rearrangement of the deprotected amine (**20**, Scheme 8). This made quantifying conversion difficult, and thus for optimization studies the consumption of **7** was tracked to assess conversion. Later, an SFC method was developed for quantifying the enantiomeric excess of **9** directly. Initial screening showed that various solvents resulted in high conversion of **7**, however TBME was favored based on the high diastereoselectivity afforded. Good ee was also obtained using TBME. Toluene performed comparably, albeit with slightly lower diastereoselectivity. It should be noted that weaker chiral bases such as $(DHQ)_2Pyr$ were also tested and did indeed form the desired adduct, however with low stereocontrol.

*Table 4. Solvent screen using chiral Brønsted base catalyst **11***

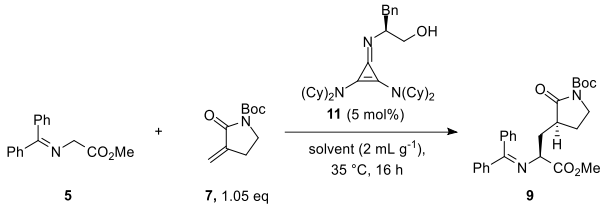

Entry	Solvent	7 at 16 h (LC-AP)	DR	%ee (*S,S*)
1	TBME	4.1	7.33 : 1	86
2	CH_2Cl_2	6.0	2.23 : 1	ND
3	EtOAc	10	2.13 : 1	ND
4	2-MeTHF	4.0	1.94 : 1	ND
5	Toluene	3.0	4.88 : 1	84

We next sought to improve the cost-effectiveness of the reaction by attempting to lower the catalyst loading (Table 5). Consumption of Michael acceptor **7** was monitored at 2 and 16 h reaction times. This analysis showed that the majority of the conversion was complete within 2 hours. At higher loadings of catalyst **11**, we observed similar results when tracking consumption of **7**, but the conversions slightly decreased at 3 mol% and below. Reducing the catalyst loading had minimal effect on the DR of the reaction. Performing the reaction on a 5g scale with 5 mol% catalyst, only 3% LC-AP of **7**, which was used in excess, remained after 16 h. Under conditions which afforded incomplete conversion at 16 h, the reactions appeared to be stalling as minimal further conversion was observed at later time points.

*Table 5: Effect of loading of catalyst **11** on conversion of **7** and DR*

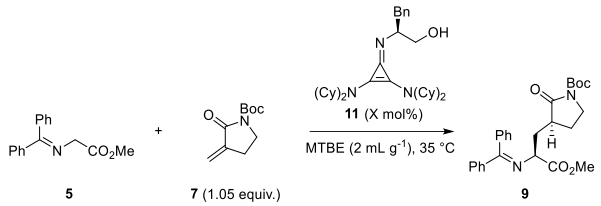

Entry	11 (mol%)	7 (LC-AP, 2 h)	7 (LC-AP, 16 h)	DR (16 h)
1	10	4.5	3.5	6.87 : 1
2	5	4.7	4.1	7.33 : 1
3	4	4.4	3.0	6.87 : 1
4	3	7.0	5.5	6.81 : 1
5	2	9.3	6.6	6.75 : 1
6	1	13.6	12.2	6.41 : 1
7	5 (5g scale)	n/a	2.7	6.69 : 1

In order to achieve full conversion with lower catalyst loading, we next explored reaction temperature and concentration effects (Table 6). Increasing the reaction temperature from 35 °C to 55 °C while using 2 mol% of **11** resulted in almost complete conversion being observed at 2 h, however a reduced DR of 4.29 : 1 was observed, compared to 6.81 : 1 at 35 °C. At 1 mol% catalyst loading at 35 °C, conversion was incomplete after 16 h, however by increasing the concentration to 3 mL g^{-1} and increasing the temperature to 40-45 °C, complete conversion was achieved with a less severe reduction in DR (5.80 : 1).

Table 6: Effect of catalyst loading, concentration and reaction temperature on conversion of 7 and DR

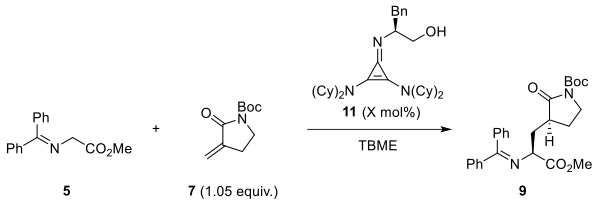

Entry	11 (mol %)	Conc (ml g^{-1})	Temp (° C)	7 (LC-AP, 2 h)	7 (LC-AP, 16 h)	DR (16 h)
1	2	5	35	9.3	6.6	6.81 : 1
2	2	5	55-60	3.5	3.2	4.29 : 1
3	2	2	55-60	3.5	2.8	4.15 : 1
4	1	5	35	13.6	12.2	n/a
5	1	5	55-60	12.0	11.0	n/a
6	1	3	40-45	4.6	3.7	5.80 : 1

The scalability of this chemistry was demonstrated using 7 g of **5** and 2 mol% of catalyst **11**, followed by a telescoped deprotection/resolution to afford **(*S,S*)-10·(-)-CSA** in 66% yield (Scheme 5).

*Scheme 5: Scale-up of synthesis of **(S,S)-10·(-)-CSA** using asymmetric Brønsted base catalysis*

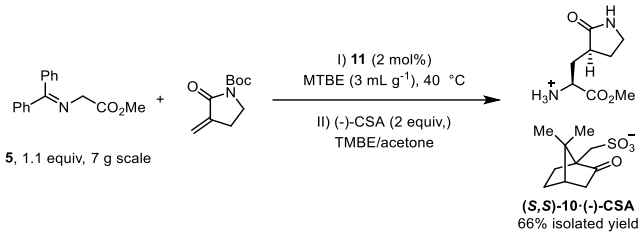

Bifunctional Hydrogen-Bond-Donor Catalysis

In addition to Brønsted base catalysis, Medicines for All Institute also investigated asymmetric bifunctional hydrogen-bond-donor (HBD) catalysts. These catalysts have been shown to be competent in controlling the stereochemistry of Michael additions with nitroalkane pro-nucleophiles.[28] Control over both α- and β- stereocenters (relative to the nitro group) in Michael adducts has been demonstrated, however without stereocontrol at the γ-position (Scheme 6A).[29] Nitroacetate pro-nucleophiles have also been used in Michael additions under bifunctional HBD catalysis, however achieving control at the α stereocenter with such nucleophiles is difficult, presumably due to epimerization at the acidic α-carbon (Scheme 6B).[30] We therefor anticipate controlling both the α- and γ-positions with a nitroacetate pro-nucleophile could be challenging, but that after nitroacetate reduction, separation of the less configurationally labile amino ester diastereomers would provide access to the core structure of fragment **3**.

Scheme 6: Bifunctional Hydrogen-Bond-Donor Catalysed Michael Addition of nitro compounds

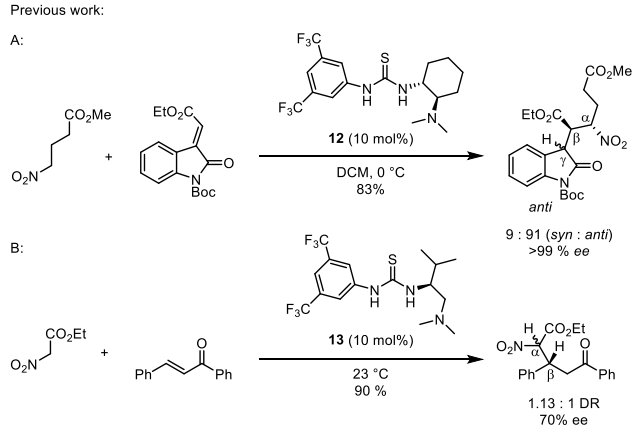

We started our investigation by testing various catalysts in the reaction between Michael acceptor **7** and methyl nitroacetate **14a** (Table 7).[1] The non-enantioselective reaction was carried out by the action of triethylamine alone, providing adduct **15a** with full conversion (by qNMR) to give a nearly 1:1 mixture of diastereomers (Entry 1). We then turned our attention to bifunctional HBD catalysts (**12**, **16**, and **17**). Utilizing the chiral thiourea catalyst **(*R,R*)-12** (at 10 mol%), we observed rapid reactivity under ambient conditions to provide **15a** with full conversion (qNMR) in -69% ee as a near equal mixture of diastereomers (Entry 2). While we did not definitively assign which of the two stereocenters is controlled in the reaction, we suspect it

to be that in the pyrrolidinone ring, as that α to the nitro group is likely to be highly labile. We then evaluated squaramide based catalyst **(*S,S*)-16**, which afforded a reduced ee of 36% (Entry 4). However the more reactive chiral squaramide **(*S,S*)-17**, featuring the same 3,5-bis(trifluoromethyl)aniline moiety as **12**, afforded both excellent reactivity and enantioselectivity, providing **15a** with full conversion in 2 hours, in 89% ee and 55:45 dr (Entry 5).

Further optimization was conducted with **(*S,S*)-17** due to its higher enantioselectivity and reactivity (shorter duration to reach reaction completion). We next looked at the effect of solvent, and found that 2-MeTHF gave superior reactivity, with complete consumption of **7** observed within 30 minutes, while maintaining high enantioselectivity (Table 2, Entry 6). Reducing catalyst loadings, however, greatly increased the time required for the reaction to reach completion, from 30 min at 10 mol% to over 24 h at 1 mol% when running the reaction at room temperature. We then found that increasing the reaction temperature to 40 °C was sufficient for completing the reaction within 24 hour using 1 mol% of catalyst, providing **15a** in 54:46 DR and 88% ee (Entry 8).

Table 7. Optimization of asymmetric bifunction HBD catalyzed Michael addition of nitroacetates into 7

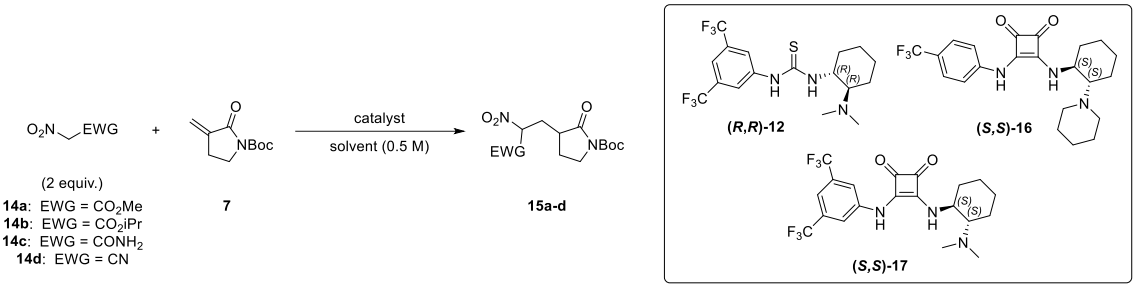

Entry	EWG	Catalyst (mol%)	Solvent	Temp (°C)	Time	DR	%ee (*S,S*)
1	CO_2Me [1]	NEt_3	DCM	rt	2 h	1.22 : 1	0
2	CO_2Me	**(*R,R*)-12** (10)	DCM	rt	6 h	1.27 : 1	-69
3	CO_2Me	**(*R,R*)-12** (10)	Toluene	rt	6 h	1.38 : 1	-66
4	CO_2Me	**(*S,S*)-16** (10)	DCM	rt	6 h	1.33 :1	36
5	CO_2Me	**(*S,S*)-17** (10)	DCM	rt	2 h	1.22 : 1	89
6	CO_2Me	**(*S,S*)-17** (10)	2-MeTHF	rt	30 min	1 : 1	89
7	CO_2Me	**(*S,S*)-17** (10)	2-MeTHF	40 °C	1.5 h	1.22 : 1	90
8	CO_2Me	**(*S,S*)-17** (1)	2-MeTHF	40 °C	24 h	1.17 : 1	88
9 [2]	CO_2Me	**(*S,S*)-17** (1)	2-MeTHF	40 °C	24 h	1.22 : 1	85
10 [3]	CO_2Me	**(*S,S*)-17** (1)	2-MeTHF	40 °C	24 h	1.17 : 1	86
11	$CO_2{}^iPr$	**(*S,S*)-17** (1)	2-MeTHF	40 °C	24 h	1.33 : 1	83
12	$CONH_2$	**(*S,S*)-17** (1)	2-MeTHF	40 °C	24 h	1 : 1	63
13	CN	**(*S,S*)-17** (1)	2-MeTHF	40 °C	24 h	ND [4]	

*Unless otherwise stated, each reaction in the above table proceeded with complete conversion of **7** by NMR. [1]Using 5 equiv. of methyl nitroacetate; [2] Reaction run with 1.3 equiv. of methyl nitroacetate, complete conversion of **7** by NMR, 95% isolated yield of the stereoisomeric mixture was obtained after workup and column purification; [3] Reaction run with 1.1 equiv. of methyl nitroacetate showed >95% conversion of SM to product,but did show some remaining SM after 24 h; [4] Reaction with nitrile showed very little conversion to product.*

In attempts to reduce the cost of this reaction further, we evaluated lowering the equivalent of methyl nitroacetate **14a** (Entries 9 and 10). We found that 1.3 equivalents was still sufficient to drive the reaction to completion, however, 1.1 equivalents resulted in detectable amounts of **7** remaining after 24 h. In an attempt to improve the DR, we tested use of the bulkier *i*-propyl nitroacetate **14b**, however did not observe any improved selectivity (Entry 11). This could be due to epimerization at the acidic α position.

Next we briefly looked at alternative activated nitromethylene nucleophiles that could be similarly used to access key starting material **3**, and obtained encouraging results with the primary amide nucleophile **14c**, albeit at reduced enantioselectivity (Entry 12). We also looked at nitroacetonitrile **14d** as a nucleophile, but found that the reaction provided very low conversion to product and thus we did not explore this further (Entry 13). Given the superior reactivity and commercial availability of methyl nitroacetate as the nucleophile, we opted to advance **14a** in our synthesis of **3**. However, further optimization using primary amide pro-nucleophile **14c** could merit further investigation in the future, as it could provide a shorter route to fragment **3.**

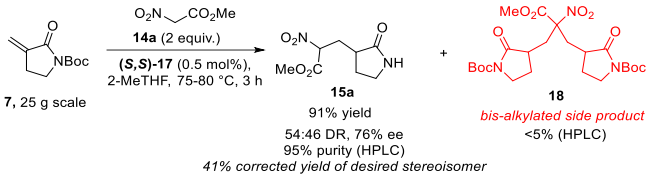

*Scheme 7. Optimized scale-up of asymmetric Michael Addition of methyl nitroacetate and **7***

We next turned our attention to scaling up and further optimizing the reaction of methyl nitroacetate **14a** and Michael acceptor **7**. Process safety testing of methyl nitroacetate highlighted some thermal stability concerns. The DSC showed an exotherm from 161 °C at -2291 J g^{-1}, indicating a high severity event[25] which is common for nitro-based compounds.[31] Six trials were conducted using the BAM Falhammer test apparatus with an impact energy of 60 J, showing no reaction overall, indicating the compound is unlikely to be shock sensitive.

For scale up experiments, we aimed to drive down the catalyst loading as much as possible, as the catalyst was a significant cost driver. At 25 g scale, we used 0.5 mol% of **(*S,S*)-17** and observed noticeably slower reaction rates. At 1.3 equivalents of methyl nitroacetate, not only was the reaction slower, but the bis-alkylated side product **18** was also found to be a significant contributor to the final reaction profile (>10% of the mixture by LC-AP). When 2 equivalents of methyl nitroacetate were used in a 25 g scale reaction, the progress was faster and the side product was observed in reduced quantities (<5% by LC-AP, Scheme 7). We also found that performing the reaction at reflux facilitated reaction progression at low catalyst loading, however a reduction in ee to 76% was observed.

With sufficient quantities of **15a** in hand, we turned our attention to advancing towards key starting material **3** (Scheme 8). We first reduced the nitro group by hydrogenation, but quickly found that the liberated free amine **19** undergoes facile rearrangement by reaction with the imide carbonyl to give the lactam **20**. In order to suppress this reaction, the Boc-group of **15a** needs to be removed first to afford the less electrophilic lactam **21**, which can be prepared in 83% yield by treatment with TFA, followed by purification by simple precipitation. Next, the nitro group of **21** was reduced by hydrogenation. In this case, no rearrangement product was observed, furnishing product **10** in 93% yield. The crude **10** was advanced to the resolution step without further purification, and treatment with (-)-CSA provided ***(S,S)*-10·(-)-CSA** in a 34% isolated yield after recrystallization.

Scheme 8**. Advancement of Michael adduct **15a** to **(S,S)-10·(-)-CSA

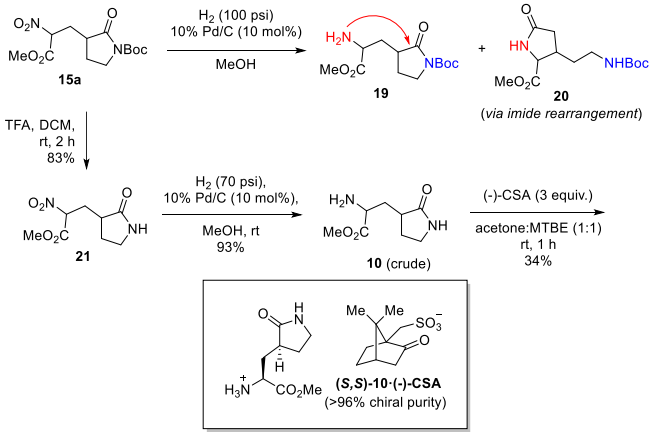

Comparison of Approaches and Conclusion

Over the course of exploring the various asymmetric approaches described, a few significant advantages of using the methyl glycine imine **5** chemistry over using the methyl nitroacetate **14a** chemistry became apparent; i) **5** is lower in cost and available in greater supply than **14a**, ii) **5** has a more favorable safety profile than **14a** based on DSC analysis and iii) adduct **9** derived from **5** is already in the correct oxidation state to advance towards **3**, unlike the adduct derived from nitroacetate **14a**. In addition, while enantioselectivity could be controlled using **14a**, no control of diastereoselectivity was observed under the conditions investigated. This is likely due to the configurational lability of the carbon α to the nitro group in adducts derived from **14a**. In contrast, reaction of **7** under both copper catalysis, and chiral Brønsted base catalysis proceeded with diastereocontrol, the latter approach offering higher levels of control than the former. However, copper catalysis enabled higher levels of control of enantioselectivity under the conditions tested. Considering the scalability of these two approaches, it's conceivable that the copper catalyzed approach may require more stringent low-oxygen conditions to avoid catalyst oxidation, and therefore may be more capricious, however this is yet to be determined. Both the copper catalyzed approach and the chiral Brønsted acid approach were developed using 1 mol% catalyst, however in both cases the catalyst was still the key cost driver.

In conclusion, we have disclosed our efforts optimizing three different catalytic asymmetric methods for setting the two non-adjacent stereocenters in a key building block for Nirmatrelvir. Use of either Cu/FesulPhos or cyclopropenimine **11** resulted in high levels of enantiocontrol and moderate diastereocontrol, enabling multigram scale preparation of **10**, a precursor to 3.[8] These methods each avoid use of cryogenic conditions and LiHMDS, which are limitations of the established chiral pool approach to this fragment.

AUTHOR INFORMATION

Corresponding Author

*Robert Szpera can be reached at robert.szpera@pfizer.com
*Robert Walton can be reached at robert.walton@pfizer.com
*Charles S. Shanahan can be reached at charles.s.shanahan@haleon.com

ACKNOWLEDGMENT

We acknowledge and thank IntelliSyn, who performed significant optimization on the chiral Brønsted base catalysed approach.

REFERENCES

1. Lamb, Y. N., Nirmatrelvir Plus Ritonavir: First Approval. *Drugs* **2022,** *82* (5), 585-591.
2. https://www.pfizer.com/news/press-release/press-release-detail/pfizer-receives-us-fda-emergency-use-authorization-novel.
3. https://www.fda.gov/media/155050/download.
4. Owen, D. R.; Allerton, C. M. N.; Anderson, A. S.; Aschenbrenner, L.; Avery, M.; Berritt, S.; Boras, B.; Cardin, R. D.; Carlo, A.; Coffman, K. J.; Dantonio, A.; Di, L.; Eng, H.; Ferre, R.; Gajiwala, K. S.; Gibson, S. A.; Greasley, S. E.; Hurst, B. L.; Kadar, E. P.; Kalgutkar, A. S.; Lee, J. C.; Lee, J.; Liu, W.; Mason, S. W.; Noell, S.; Novak, J. J.; Obach, R. S.; Ogilvie, K.; Patel, N. C.; Pettersson, M.; Rai, D. K.; Reese, M. R.; Sammons, M. F.; Sathish, J. G.; Singh, R. S. P.; Steppan, C. M.; Stewart, A. E.; Tuttle, J. B.; Updyke, L.; Verhoest, P. R.; Wei, L.; Yang, Q.; Zhu, Y., An oral SARS-CoV-2 M(pro) inhibitor clinical candidate for the treatment of COVID-19. *Science* **2021,** *374* (6575), 1586-1593.
5. US 20220062232A1 NITRILE - CONTAINING ANTIVIRAL COMPOUNDS.
6. Algera, R. F.; Allais, C.; Baldwin, A. F.; Becirovic, H.; Bowles, P.; Brown, A. R.; Buske, J. M.; Clarke, H. J.; Do, N. M.; Doyle, K.; Fifer, J.; Gray, K.; Happe, A.; Hardink, M.; Hubbell, A. K.; James, C.; Khadamkar, H. P.; Magano, J.; McInturff, E. L.; Mustakis, J.; Ozbuyukkaya, G.; Piper, J. L.; Place, D. W.; Ragan, J. A.; Rauschenberger, B.; Reyes, G.; Shehadeh, R.; Stanchina, C.; Stanley, M.; Weekly, R. M.; Weinstein, E.; Weisenburger, G. A.; Wood, E.; Yayla, H. G.; Yu, S., Synthesis of Nirmatrelvir: Development of an Efficient, Scalable Process to Generate the Western Fragment. *Organic Process Research & Development* **2023**.
7. Algera, R. F.; Allais, C.; Baldwin, A. F.; Busch, T.; Colombo, F.; Colombo, M.; Depretz, C.; Dumond, Y. R.; Faria Quintero, A. R.; Heredia, M.; Jung, J.; Lall, A.; Lee, T.; Liu, Y.; Mandelli, S.; Mantel, M.; Morris, R.; Mustakis, J.; Nguyen, B.; Pearson, R.; Piper, J. L.; Ragan, J. A.; Ruffin, B.; Talicska, C.; Tcyrulnikov, S.; Uyeda, C.; Weekly, R. M.; Zeng, M., Synthesis of Nirmatrelvir: Development of a Scalable Cobalt-Catalyzed Cyclopropanation for Manufacture of the Bicyclic [3.1.0]Proline-Building Block. *Organic Process Research & Development* **2023**.
8. Algera, R. F.; Allais, C.; Becirovic, H.; Brown, A. R.; Chen, B.; Clarke, H. J.; Concannon, P. E.; Du, Y.; Georgian, W.; Lee, J. W.; Lee, T.; Magano, J.; Perez Mandry, C.; Mehta, R.; Mull, E.; Pearson, R.; Peng, Z.; Piper, J. L.; Ragan, J. A.; Reyes, G.; Shen, H.; Ward, D. W.; Weekly, R. M.; Weisenburger, G. A.; Xu, P.; Yayla, H. G.; Zhang, M., Synthesis of Nirmatrelvir: Development of Magnesium Sulfate-Mediated Aminolysis for the Manufacture of the Eastern Fragment. *Organic Process Research & Development* **2023**.
9. Algera, R. F.; Baldwin, A. F.; Bowles, P.; Clarke, H. J.; Connor, C. G.; Cordi, E. M.; Do, N. M.; Nicholson, L. D.; Georgian, W.; Happe, A.; Herman, M. I.; Hilou, E.; James, C.; Johnson, A. M.; Kalinowski, M.; Kulkarni, S. A.; Launer-Felty, K. D.; Lee, J. W.; Lee, T.; Lopez, J.; McInturff, E. L.; Piper, J. L.; Place, D. W.; Ragan, J. A.; Rauschenberger, B.; Ryder, K.; Stanley, M.; Weisenburger, G. A.; Weekly, R. M.; Allais, C., Synthesis of Nirmatrelvir: Design and Optimization of an Efficient Telescoped Amidation–Dehydration Sequence. *Organic Process Research & Development* **2023**.
10. Hanessian, S.; Margarita, R., 1,3-Asymmetric induction in dianionic allylation reactions of amino acid derivatives-synthesis of functionally useful enantiopure glutamates, pipecolates and pyroglutamates. *Tetrahedron Letters* **1998,** *39* (33), 5887-5890.
11. Hanessian, S.; Schaum, R., 1,3-Asymmetric induction in enolate alkylation reactions of N-protected γ-amino acid derivatives. *Tetrahedron Letters* **1997,** *38* (2), 163-166.
12. Tian, Q.; Nayyar, N. K.; Babu, S.; Chen, L.; Tao, J.; Lee, S.; Tibbetts, A.; Moran, T.; Liou, J.; Guo, M.; Kennedy, T. P., An efficient synthesis of a key intermediate for the preparation of the rhinovirus protease inhibitor AG7088 via asymmetric dianionic cyanomethylation of N-Boc-l-(+)-glutamic acid dimethyl ester. *Tetrahedron Letters* **2001,** *42* (39), 6807-6809.
13. Vuong, W.; Vederas, J. C., Improved Synthesis of a Cyclic Glutamine Analogue Used in Antiviral Agents Targeting 3C and 3CL Proteases Including SARS-CoV-2 M(pro). *J Org Chem* **2021,** *86* (18), 13104-13110.
14. Qin, H.; Jin, C.; Odilov, A.; Mintah Bonku, E.; Zhu, F.; Liu, Q.; Shen, J.; Aisa, H. A., Optimized Synthesis of a Key Intermediate of Nirmatrelvir. *Organic Process Research & Development* **2022,** *27* (1), 78-83.
15. Strohmeier, M.; Leach, K.; Zajac, M. A., Asymmetric conjugate addition of glycine derivatives under copper catalysis. *Angew Chem Int Ed Engl* **2011,** *50* (51), 12335-8.
16. Liu, B.; Zhang, Z.-M.; Xu, B.; Xu, S.; Wu, H.-H.; Liu, Y.; Zhang, J., Cu(i)-catalyzed Michael addition of ketiminoesters to β-trifluoromethyl β,β-disubstituted enones: rapid access to 1-pyrrolines bearing a quaternary all-carbon stereocenter. *Organic Chemistry Frontiers* **2017,** *4* (9), 1772-1776.
17. Hernandez-Toribio, J.; Arrayas, R. G.; Carretero, J. C., Enantiocontrolled synthesis of beta-branched alpha-amino acids by using Cu(I) -catalyzed 1,4-addition of glycine imines to beta-substituted gem-diactivated olefins. *Chemistry* **2011,** *17* (23), 6334-7.
18. Konno, T.; Watanabe, S.; Takahashi, T.; Tokoro, Y.; Fukuzawa, S., Silver/ThioClickFerrophos complex as an effective catalyst for asymmetric conjugate addition of glycine imino ester to unsaturated malonates and alpha-enones. *Org Lett* **2013,** *15* (17), 4418-21.
19. Tsubogo, T.; Saito, S.; Seki, K.; Yamashita, Y.; Kobayashi, S., Development of catalytic asymmetric 1,4-addition and [3 + 2] cycloaddition reactions using chiral calcium complexes. *J Am Chem Soc* **2008,** *130* (40), 13321-32.
20. Kobayashi, S.; Tsubogo, T.; Saito, S.; Yamashita, Y., Calcium-catalyzed diastereo- and enantioselective 1,4-addition of glycine derivatives to alpha,beta-unsaturated esters. *Org Lett* **2008,** *10* (5), 807-9.
21. Hut'ka, M.; Tsubogo, T.; Kobayashi, S., Synthesis of Glutamic Acid and Highly Functionalized Pyrrolidine Derivatives by Utilizing Tunable Calcium Catalysts for Chemoselective Asymmetric 1,4-Addition and [3+2] Cycloaddition Reactions. *Advanced Synthesis & Catalysis* **2013,** *355* (8), 1561-1569.
22. Cabrera, S.; Gomez Arrayas, R.; Carretero, J. C., Highly enantioselective copper(I)-fesulphos-catalyzed 1,3-dipolar cycloaddition of azomethine ylides. *J Am Chem Soc* **2005,** *127* (47), 16394-5.
23. Llamas, T.; Arrayás, R. G.; Carretero, J. C., Catalytic Enantioselective 1,3-Dipolar Cycloaddition of Azomethine Ylides with Vinyl Sulfones. *Organic Letters* **2006,** *8* (9), 1795-1798.

24. Yildirim, O.; Grigalunas, M.; Brieger, L.; Strohmann, C.; Antonchick, A. P.; Waldmann, H., Dynamic Catalytic Highly Enantioselective 1,3-Dipolar Cycloadditions. *Angew Chem Int Ed Engl* **2021,** *60* (36), 20012-20020.
25. Stoessel, F., *Thermal Safety of Chemical Processes*. 2008.
26. Bandar, J. S.; Barthelme, A.; Mazori, A. Y.; Lambert, T. H., Structure–activity relationship studies of cyclopropenimines as enantioselective Brønsted base catalysts. *Chemical Science* **2015,** *6* (2), 1537-1547.
27. Bandar, J. S.; Lambert, T. H., Enantioselective Bronsted base catalysis with chiral cyclopropenimines. *J Am Chem Soc* **2012,** *134* (12), 5552-5.
28. Ballini, R.; Palmieri, A.; Petrini, M., Catalysts' evolution in the asymmetric conjugate addition of nitroalkanes to electron-poor alkenes. *Organic Chemistry Frontiers* **2022,** *9* (21), 6077-6113.
29. Quintavalla, A.; Lanza, F.; Montroni, E.; Lombardo, M.; Trombini, C., Organocatalytic conjugate addition of nitroalkanes to 3-ylidene oxindoles: a stereocontrolled diversity oriented route to oxindole derivatives. *J Org Chem* **2013,** *78* (23), 12049-64.
30. Manzano, R.; Andres, J. M.; Alvarez, R.; Muruzabal, M. D.; de Lera, A. R.; Pedrosa, R., Enantioselective conjugate addition of nitro compounds to alpha,beta-unsaturated ketones: an experimental and computational study. *Chemistry* **2011,** *17* (21), 5931-8.
31. Maule, I.; Razzetti, G.; Restelli, A.; Palmieri, A.; Colombo, C.; Ballini, R., Thermal Stability Evaluation of Nitroalkanes with Differential Scanning Calorimetry. *Organic Process Research & Development* **2021,** *25* (4), 781-788.